Tetrahedron 64 (2008) 8553–8557

Contents lists available at ScienceDirect

Tetrahedron

journal homepage: www.elsevier.com/locate/tet

Room temperature synthesis of metal-organic frameworks: MOF-5, MOF-74, MOF-177, MOF-199, and IRMOF-0

David J. Tranchemontagne, Joseph R. Hunt, Omar M. Yaghi *

Center for Reticular Chemistry at California NanoSystems Institute, Department of Chemistry and Biochemistry, University of California, Los Angeles, CA 90095-1569, USA

ARTICLE INFO

Article history:
Received 3 June 2008
Received in revised form 9 June 2008
Accepted 11 June 2008
Available online 14 June 2008

ABSTRACT

Room temperature synthesis of metal-organic frameworks (MOFs) has been developed for four well-known MOFs: MOF-5, MOF-74, MOF-177, and MOF-199. A new isoreticular metal framework (IRMOF), IRMOF-0, having the same cubic topology as MOF-5, has been synthesized from acetylenedicarboxylic acid using this method to accommodate the thermal sensitivity of the linker. Despite acetylenedicarboxylate being the shortest straight linker that can be made into an IRMOF, IRMOF-0 forms as a doubly interpenetrating structure, owing to the rod-like nature of the linker.

1. Introduction

Metal-organic frameworks (MOFs) represent a new class of porous crystalline materials for which it is possible to design organic linkers and inorganic joints.[1] A class of MOFs, isoreticular MOFs (IRMOF) share a common cubic topology constructed from linear organic links connecting Zn_4O clusters as in MOF-5 (i.e., IRMOF-1).[2,3] Over 12,000 MOF structures have been reported in the CSD as of 2005, with the number of 3D MOFs doubling every 3.9 years.[4] This intense research focus has concentrated on their synthesis and the study of their gas adsorption properties for hydrogen/methane storage, carbon dioxide capture, gas separations, and catalysis,[5,6] and more recently investigation of chemical modification and impregnation of MOFs.[7,8] Increasing effort is being put forth to investigate the synthesis, physical properties, and chemical properties to better understand how to use MOFs for these applications.[9]

The synthesis of MOFs is frequently performed by solvothermal methods: heating a mixture of organic linker and metal salt in a solvent system that usually contains formamide functionality. These methods often yield crystals suitable for single crystal X-ray diffraction analysis, but have the obvious disadvantage of being relatively slow (hours to weeks). Furthermore, solvothermal conditions are unsuitable for thermally sensitive starting materials.

MOF-5, originally described in 1999, consists of Zn_4O units connected by linear 1,4-benzenedicarboxylate struts to form a cubic network.[2] Several isoreticular (sharing a common net topology) MOFs, all with the same cubic construction as MOF-5, have been synthesized, with the first series of these reported in 2002.[3] Here we show that heating the reaction is not necessary to produce highly crystalline MOFs. We illustrate this by the synthesis of both known MOFs and new MOFs. For example, syntheses have been demonstrated for MOF-5 in which the starting materials are mixed in solution at ambient temperature. Subsequent addition of triethylamine causes deprotonation of the organic linker to precipitate MOF-5. Base addition can either be done slowly by diffusion (as described in the original synthesis of MOF-5)[2] or rapidly as an aliquot.[10] The former frequently yields MOF single crystal mixtures, which must be mechanically separated, whereas the latter method yields MOFs as microcrystalline powders.

The ambient temperature synthesis conditions described above, particularly with fast addition of base, are easy to scale up, but the use of zinc nitrate poses potential safety concerns, especially for large-scale production. Furthermore, reports of such synthetic conditions have been largely limited to MOF-5 and IRMOF-8.[10–12]

Here we report rapid, simple, and high yielding room temperature syntheses for some important MOFs: MOF-5, MOF-74, MOF-177, and MOF-199 (HKUST-1) (Fig. 1). These MOFs were chosen because they represent a cross-section of desirable properties such as ultrahigh porosity (MOF-5 and MOF-177), one dimensional pores (MOF-74), and open metal sites (MOF-74 and MOF-199); attributes that have implications in high storage capacities of hydrogen and methane. We demonstrate that these synthetic methods work well for Cu(II) and Zn(II) containing MOFs. We illustrate the usefulness of this method for the synthesis of new MOFs by synthesizing an IRMOF, IRMOF-0, which uses acetylenedicarboxylate as the link. This is the shortest linear link that can be used to make an IRMOF; oxalic acid is known to react with zinc to make extended structures, but does not form the octahedral zinc cluster.[13]

* Corresponding author.
E-mail address: yaghi@chem.ucla.edu (O.M. Yaghi).

0040-4020/$ – see front matter © 2008 Elsevier Ltd. All rights reserved.
doi:10.1016/j.tet.2008.06.036

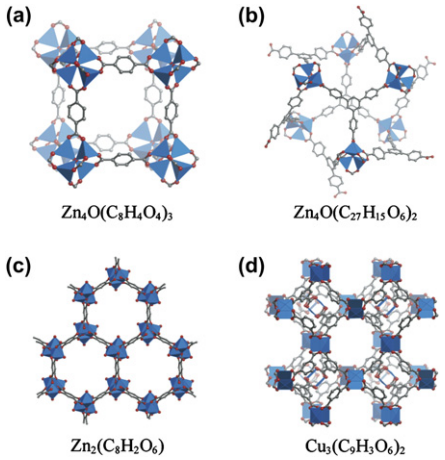

Figure 1. Important MOFs chosen for generalized synthesis: (a) MOF-5, (b) MOF-177, (c) MOF-74, and (d) MOF-199. These MOFs contain metal-oxide SBUs (secondary building units) that are 0D: $Zn_4O(CO_2)_6$ (MOF-5 and MOF-177) and $Cu_2(CO_2)_4$ with coordinatively unsaturated Cu(II) centers (MOF-199); and 1D: $Zn_3[(O)_3(CO_2)_3]$ with coordinatively unsaturated Zn(II) sites (MOF-74). C, gray; O, red; Zn; and Cu, blue.

2. Results and discussion

MOF-5 was prepared using a room temperature synthesis, wherein separate *N*,*N*-dimethylformamide (DMF) solutions of terephthalic acid with triethylamine and zinc acetate dihydrate were prepared, then the zinc salt solution was added to the organic solution with rapid stirring at ambient temperature. A white precipitate was observed almost immediately and the reaction was allowed to proceed for 2.5 h. Analysis of the resulting material by X-ray powder diffraction (XRPD) revealed that the solid was pure MOF-5 by comparison with the pattern simulation from the crystal structure (Fig. 2a).

The MOF-5 synthesis reaction was repeated without addition of base, using zinc acetate dihydrate, and the mixture was stirred for only 45 min, again yielding pure MOF-5 (Fig. 2a). This demonstrates that the addition of triethylamine as a base is unnecessary when zinc acetate is used as a source of Zn(II) in the MOF-5 synthesis.

MOF-74[14] and MOF-177[15] were prepared in a similar manner (see Section 4). Zinc acetate dihydrate and the respective organic starting material were combined in a vial and stirred together in DMF overnight. The product of each reaction was collected and the XRPD pattern for each is consistent with simulated patterns of the solvothermally synthesized MOFs crystal structures (Fig. 2b and c). This general procedure was also used to synthesize MOF-199,[16] using benzenetricarboxylic acid, copper acetate monohydrate, 1:1:1 DMF/EtOH/H_2O, and triethylamine, yielding pure crystalline MOF (Fig. 2d).

To establish that this synthetic method does indeed produce porous microcrystalline MOF powders, MOF-5, MOF-74, and MOF-177 were activated by solvent exchange with appropriate volatile solvent, followed by heating under vacuum.[17] Their surface areas were calculated from N_2 adsorption isotherm data obtained using a Quantachrome Nova surface area analyzer (Fig. 3).

Langmuir surface areas were found to be 3909 m^2/g, 1187 m^2/g, and 4944 m^2/g for MOF-5, MOF-74, and MOF-177, respectively. These values are consistent with previously reported surface areas.[7] From these data, in conjunction with powder diffraction, we show that we can use room temperature synthetic methods to

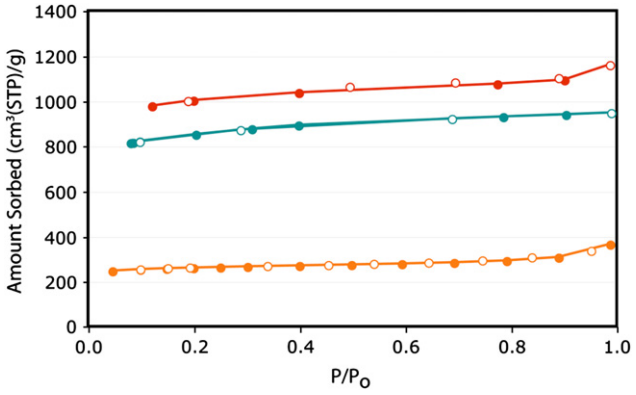

Figure 3. N_2 isotherms for room temperature-synthesized MOF-5 (green), MOF-74 (orange), and MOF-177 (red) at 77 K. Adsorption data are shown as closed circles and desorption data as open circles.

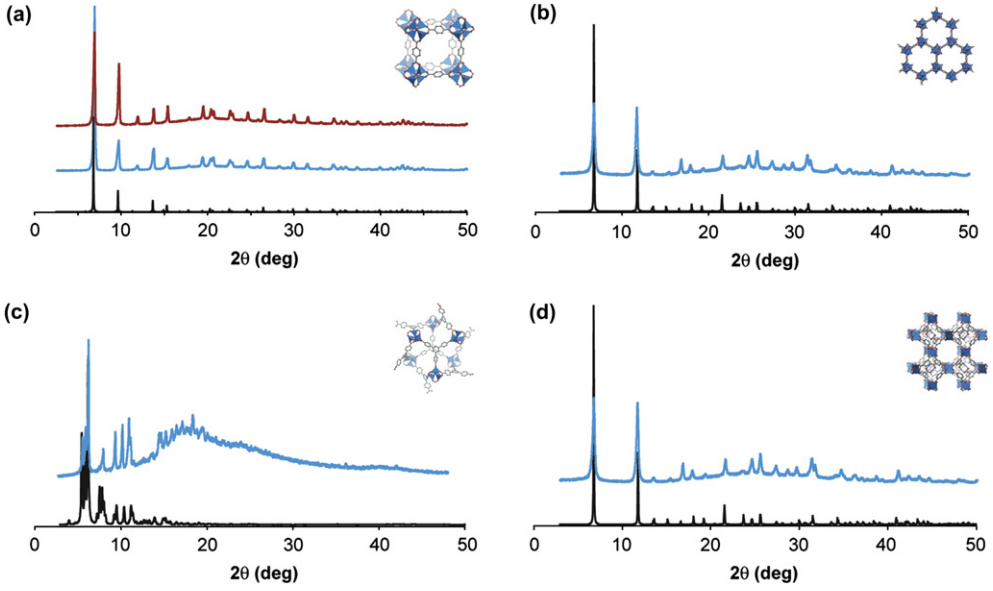

Figure 2. Powder patterns of (a) MOF-5, (b) MOF-74, (c) MOF-177, and (d) MOF-199. Simulated patterns are in black, experimental patterns of as-synthesized MOFs are in blue. In (a) the blue and red traces correspond to the synthesis with $Zn(NO_3)_2{\cdot}4H_2O$, $Zn(OAc)_2{\cdot}2H_2O$, respectively.

successfully synthesize the same porous MOFs we have previously synthesized with solvothermal methods, but more quickly.

Having demonstrated the utility of this method toward MOF synthesis, we then turned toward the synthesis of IRMOF-0, containing acetylenedicarboxylate as the link. The greatest setback faced when attempting to synthesize IRMOF-0 is the thermal sensitivity of acetylenedicarboxylic acid in solution. Acetylenedicarboxylic acid is known to decompose upon heating.[18] By contrast, MOF-31 has been synthesized using room temperature conditions.[19] They combined acetylenedicarboxylic acid with zinc nitrate in ethanol, and used triethylamine vapor-diffusion to deprotonate the link and form an augmented diamond framework; the product is composed of two interpenetrating frameworks.

Knowing the synthetic conditions used to make MOF-5 at room temperature and those used to make MOF-31, IRMOF-0 was synthesized by dissolving acetylenedicarboxylic acid and zinc acetate dihydrate in DMF to form a clear solution. The lack of precipitation was evidence that the acetate anion was not sufficiently basic to deprotonate the acetylenedicarboxylic acid, so triethylamine was added to the stirred solution. After a short time, a white precipitate formed, which was evaluated by PXRD, TGA, and FTIR spectroscopy.

The structure of IRMOF-0 was elucidated from the powder diffraction data and modeling of the structure using Cerius^2.[20] Acetylenedicarboxylate is a rod-like linker, making it possible for the network to interpenetrate.[21,22] To determine whether or not IRMOF-0 would interpenetrate, a model based on that of MOF-5, with the same space group (*Fm*-3*m*) and a unit cell length of a=21.84 Å, was devised; this cell length corresponds to the distance between carboxylate carbons when the link is changed from benzene to acetylene. The model considers bond lengths of acetylenedicarboxylate based on a known crystal structure of a salt of the monodeprotonated acid.[23] The bond lengths in the model are 1.19 Å for the C≡C bond and 1.44 Å for the C–C bonds. This would yield a MOF with fixed and free diameters 7.56 and 11.20 Å, respectively. Comparison between the simulated and experimental pattern showed that the material was not the expected non-interpenetrated IRMOF (Fig. 4).

A change in the space group from *Fm*-3*m* to *Fd*-3*c* (a=21.84 Å) generates a model of the interpenetrated structure. Comparison of the experimental data with the calculated pattern from this model (Fig. 5) shows that IRMOF-0 forms as a doubly interpenetrated structure (Fig. 6). We note that the peak positions match well with the model, while the relative intensities do not. In particular, the peaks at 2θ=14.04° and 16.22°, although present in the experimental pattern, appear with very low intensity. Such differences in intensities in MOFs are common because the structure is modeled in the absence of guests in the pores, while the experimental pattern is obtained in the presence of solvent and thus having guests in the pores. This affects the peak intensities, but not the positions. Elemental analysis and FTIR spectroscopy confirm the presence of guests in the pores, which are not included in the model. Because guest molecules are not taken into account, the pattern calculated from the Cerius^2 models does not reflect all of the expected peak intensities, but only peak positions. The comparison of the experimental powder patterns to the calculated models is displayed in Figure 5, where there is a close correspondence between the peak positions, substantiating that this is indeed the structure, albeit with guests not modeled. Indexing of the experimental X-ray pattern unambiguously gave unit cell parameters nearly equivalent to those determined from the models. To obtain the experimental values, we freely refined the unit cell parameters using full pattern decomposition and profile fitting of the diffraction patterns using a model-biased Le Bail routine to extract the intensities (F_{obs}) for each structure. The blue difference plot in Figure 5 indicates that the degree of fitting is acceptable for the refined profile (including unit cell parameters). [IRMOF-0: wR_p=0.1228, R_p=0.0928 (where R_p and wR_p are profile-fitting factors)].

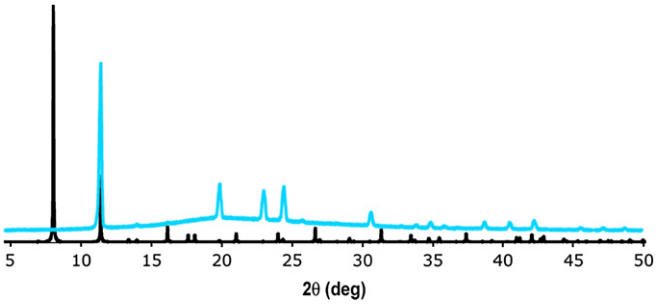

Figure 4. Simulated powder pattern of non-interpenetrated IRMOF-0 in *Fm*-3*m* (black) and the experimental powder pattern obtained (blue). Comparison shows that the MOF obtained is not a non-interpenetrated IRMOF.

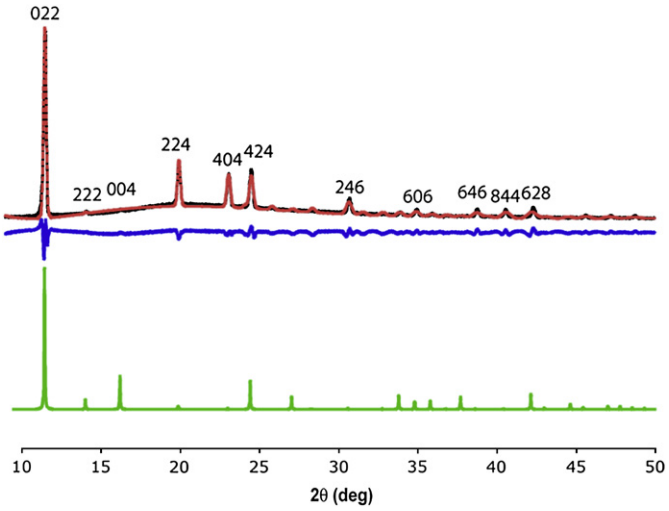

Figure 5. X-ray analysis of interpenetrated IRMOF-0 with the observed pattern in black, the refined profile in red, and the difference plot in blue (observed minus refined profiles). The green trace is the calculated PXRD pattern from Cerius^2.

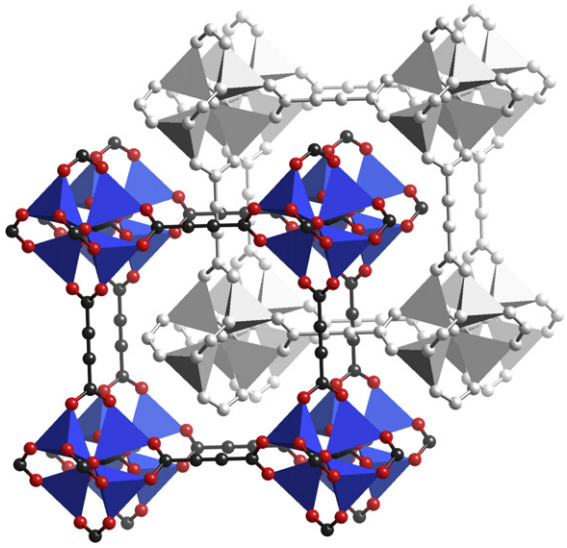

Figure 6. The structure of IRMOF-0 modeled in Cerius^2. Under the synthetic conditions used, IRMOF-0 forms as a doubly interpenetrated structure. C, black; O, red; and Zn, blue. The second interpenetrating framework is represented in gray.

Analysis of the modeled structure (Fig. 6) shows that the distance between the two interpenetrating frameworks is 5.46 Å (measured between centers of the alkynes). Because of this small distance between the frameworks, the largest sphere that can fit between the alkynes where they cross is 4.4 Å in diameter, while the pore itself has a 7.8 Å diameter; these correspond to the fixed and free diameters, respectively. This data suggests that DMF, triethylamine, water, or other guests could all fit within the pores, and are in the pores as the MOF forms, but that the interpenetration would prevent any guests within the pores from being removed. The elemental analysis of material washed 4 times with DMF and 4 times with diethyl ether, followed by evacuation, demonstrates that guest molecules do indeed still reside within the pores.

Additionally, the kinetic diameter of N_2 is 3.64 Å and that of H_2 is 2.89 Å, which could fit inside of the pore but they could not fit through the aperture. This factor, combined with guests that cannot be removed from the pores, leads to a nonporous material. Low-pressure (0–1 atm) adsorption experiments with N_2 and H_2 at 77 K confirm this, as no uptake is observed.

Thermogravimetric analysis under N_2 of a sample washed with DMF and then anhydrous Et_2O (Fig. 7) shows that IRMOF-0 decomposes at a much lower temperature than is commonly seen for IRMOFs. After solvent exchange with Et_2O, no significant weight loss is seen until 120 °C, at which point a sharp decrease indicates that decomposition occurs. IRMOF-0 begins to decompose at only 120 °C, whereas MOF-5 and other IRMOFs show stability up to 400 °C or higher. This stems from the low thermal stability of acetylenedicarboxylate. After decomposition, at 500 °C, 24.3% of the starting weight remains. This corresponds to formation of 4ZnO from the formula determined by elemental analysis, $Zn_4O(ADC)_4(Et_3N)_6$.

Additional evidence of guests trapped within the material can be seen in the FTIR spectrum of the washed and evacuated material. The spectrum shows C–H stretches, indicating that guests with alkyl chains are still present in the material. The carbonyl stretches at 1648 and 1612 cm^{-1} are at lower energies than those of acetylenedicarboxylic acid (1698 and 1690 cm^{-1}), consistent with coordination to Zn. The C≡C bond stretching vibration is symmetry forbidden.

3. Conclusion

In this study, we have shown that room temperature synthetic methods can be used to produce known and new MOFs. We have described a novel MOF (IRMOF-0) incorporating acetylenedicarboxylate as linker and displaying double interpenetration. From the modeled structure of IRMOF-0, we observe that the pore apertures are too small to allow for removal of trapped guest molecules or adsorption of gases, and both FTIR and elemental analysis indicate that guest molecules are trapped within the pores, thus precluding porosity. While this material is nonporous, it is a demonstration of these new synthetic methods toward design and synthesis of new MOFs.

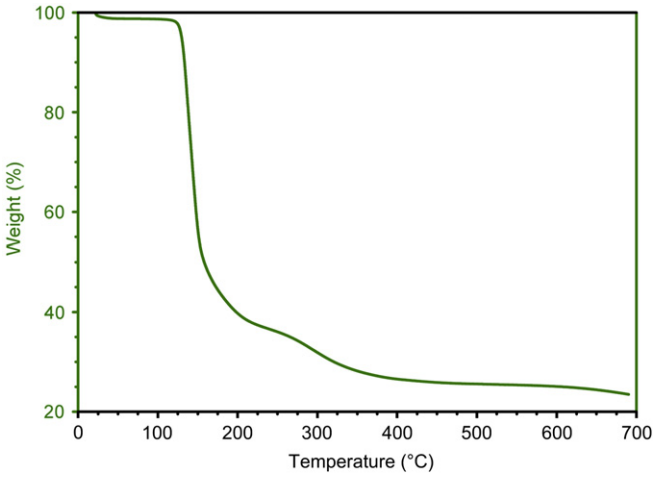

Figure 7. Thermogravimetric analysis of IRMOF-0 under N_2 after washing with DMF and Et_2O. Decomposition of the material begins sharply at 120 °C. After decomposition, at 500 °C, 24.3% percent of the weight remains, corresponding to 4 ZnO formed during decomposition of the proposed composition $Zn_4O(ADC)_4(Et_3N)_6$.

4. Experimental

4.1. Materials

Zinc acetate dihydrate ($Zn(OAc)_2\cdot 2H_2O$) was purchased from Alfa Aeasar. Acetylenedicarboxylic acid and triethylamine were purchased from Fluka. *N*,*N*-Dimethylformamide (DMF) was purchased from Fisher Scientific. All materials were used without further purification.

4.2. Instrumentation

Powder X-ray diffraction (PXRD) patterns were collected with a Bruker AXS D8 Advanced diffractometer operated at 40 kV and 40 mA with monochromated Cu Kα radiation (λ=1.5406 Å) and with a scan speed of 1 s/step and a step size of 0.05°. Structural modeling was performed on Cerius[2] software suite. The simulated PXRD patterns were calculated from modeled crystal data using the PowderCell 2.3 software suite.[24] Thermogravimetric analyses (TGA) were performed on a TA Q500 thermal analysis system with the sample held in a platinum pan in a continuous nitrogen flow atmosphere. Fourier transform infrared (FTIR) spectra were obtained by using a Nicolet FT-IR Impact 400 system and KBr pellet samples. Absorption peaks were described as follows: very strong (vs), strong (s), medium (m), weak (w), broad (br), and shoulder (sh). Elemental analysis was performed on a Thermo Scientific FlashEA 1112.

4.3. Synthesis

4.3.1. MOF-5

Terephthalic acid (5.065 g, 30.5 mmol) and triethylamine (8.5 mL) were dissolved in 400 mL of DMF. $Zn(OAc)_2\cdot 2H_2O$ (16.99 g, 77.4 mmol) was dissolved in 500 mL of DMF. The zinc salt solution was added to the organic solution with stirring over 15 min, forming a precipitate, and the mixture was stirred for 2.5 h. A sample of the mixture, still damp, was used for PXRD analysis, which showed pure MOF-5 by comparison with the pattern simulated from SXRD data (Fig. 2a).[2] The precipitate was filtered and immersed in DMF (250 mL) overnight. It was then filtered again and immersed in $CHCl_3$ (350 mL, HPLC grade). The solvent was exchanged 3 times over 7 days: after 2 days, 3 days, and 7 days. The bulk of the solvent was decanted and the product was evacuated overnight to a pressure of 10 mTorr. It was activated at 120 °C and 10 mTorr for 6 h, at which point it was transferred to a glovebox and weighed (4.92 g, 63%).

4.3.2. MOF-74

2,5-Dihydroxyterephtalic acid (239 mg, 1.20 mmol) and $Zn(OAc)_2\cdot 2H_2O$ (686 mg, 3.12 mmol) were each dissolved in 20 mL of dimethylformamide (DMF). The diacid solution was added to the stirring zinc salt solution over 10 min, and the mixture was stirred at room temperature for 18 h, at which point a sample was taken for PXRD analysis, which showed pure MOF-74 by comparison with the pattern simulated from SXRD data (Fig. 2b).[14] The product was centrifuged and the mother liquor was decanted. The product was

washed with 3×20 mL of DMF. It was then washed with 2×20 mL of methanol and immersed in methanol (20 mL) overnight. This methanol wash-immersion procedure was repeated twice more. The methanol was decanted and the MOF-74 was evacuated for 7 h at ambient temperature. Under vacuum, it was heated to 110 °C for 10 h, then to 260 °C for 12 h, after which it was cooled to room temperature over 2 h, giving a yield of 269.5 mg (69%).

4.3.3. MOF-177

Benzenetribenzoic acid (626 mg, 1.43 mmol) and $Zn(OAc)_2 \cdot 2H_2O$ (2.51 g, 11.4 mmol) were stirred in 50 mL of DEF for 3 h, at which point a sample was taken for PXRD analysis, which showed pure MOF-177 by comparison with the pattern simulated from SXRD data (Fig. 2c).[15] The product was collected by filtration, washed with 10 mL of DEF, and immersed in 40 mL of $CHCl_3$ (HPLC grade). The solvent was refreshed 3 times in 5 days: after 1 day, 4 days, and 5 days. The bulk of the solvent was decanted and the product was split into two samples, one for bulk activation and one for activation in a quartz cell for N_2 sorption. Both samples were activated under vacuum (≤10 mTorr) at 120 °C for 12 h, giving a total yield of 490 mg (60%). The bulk product was stored in the glovebox.

4.3.4. MOF-199

Benzenetricarboxylic acid (500 mg, 2.38 mmol) was mixed in 12 mL of a 1:1:1 mixture of DMF/EtOH/H_2O. $Cu(OAc)_2 \cdot H_2O$ (860 mg, 4.31 mmol) was mixed with 12 mL of the same solvent and the mixtures were combined with stirring. Triethylamine (0.5 mL) was added to the reaction mixture, which was stirred for 23 h. The product was collected by filtration and washed with 2×25 mL of DMF and a sample was collected for PXRD analysis, which showed pure MOF-199 by comparison with the pattern simulated from SXRD data (Fig. 2d).[16] The product was collected by filtration, washed with 2×25 mL of DMF, then immersed in 50 mL of CH_2Cl_2 (HPLC grade) overnight. The next day, the solvent was exchanged for fresh solvent 3 times (50 mL portions) and left overnight. It was then evacuated to ≤5 mTorr overnight, during which time the deep blue solid became blue-violet. The product was brought into the glovebox under vacuum and weighed (316 mg, 44%).

4.3.5. IRMOF-0

Acetylenedicarboxylic acid (2.01 g, 17.6 mmol) was dissolved in DMF (50 mL) and $Zn(OAc)_2 \cdot 2H_2O$ (8.00 g, 36.4 mmol) was dissolved in DMF (60 mL). The two solutions were combined with stirring. Triethylamine (5 mL) was added to the stirring mixture and the reaction was allowed to run overnight. A sample of solid was collected for PXRD analysis (Fig. 4). FTIR: 3063 (br), 2987 (m), 2951 (m), 2890 (m), 2819 (m), 2758 (m), 1648 (s), 1612 (s). The product was collected by filtration and washed with DMF (2×15 mL), then with dry Et_2O (4×15 mL, solvent purification column) and evacuated on a Schlenk line to 10 mTorr overnight. TGA of the washed, evacuated material showed decomposition starting at 120 °C (Fig. 7). Anal. Calcd for $Zn_4O(ADC)_4(Et_3N)_6$: C, 46.9; H, 6.81; N, 6.30%. Found: C, 47.0; H, 6.51; N, 6.19%.

Acknowledgements

We are grateful to Dr. Adrien P Côté for his help in modeling the structure of IRMOF-0. This work was supported by the BASF (Ludwigshafen, Germany).

References and notes

1. Yaghi, O. M.; O'Keeffe, M.; Ockwig, N. W.; Chae, H. K.; Eddaoudi, M.; Kim, J. *Nature* **2003**, *423*, 705–714.
2. Li, H.; Eddaoudi, M.; O'Keeffe, M.; Yaghi, O. *Nature* **1999**, *402*, 276–279.
3. Eddaoudi, M.; Kim, J.; Rosi, N.; Vodak, D.; O'Keeffe, M.; Yaghi, O. M. *Science* **2002**, *295*, 469–472.
4. Ockwig, N. W.; Delgado-Friedrichs, O.; O'Keefe, M.; Yaghi, O. M. *Acc. Chem. Res.* **2005**, *38*, 176–182.
5. Mueller, U.; Schubert, M.; Teich, F.; Puetter, H.; Schierle-Arndt, K.; Pastré, J. *J. Mater. Chem.* **2006**, *16*, 626–636.
6. Collins, D. J.; Zhou, H. *J. Mater. Chem.* **2007**, *17*, 3154–3160.
7. Wang, Z.; Cohen, S. M. *J. Am. Chem. Soc.* **2007**, *129*, 12368–12369.
8. Kaye, S. S.; Long, J. R. *J. Am. Chem. Soc.* **2008**, *130*, 806–807.
9. Kitagawa, S.; Kitaura, R.; Noro, S. *Angew. Chem., Int. Ed.* **2004**, *43*, 2334–2375.
10. Li, Y.; Yang, R. T. *J. Am. Chem. Soc.* **2006**, *128*, 726–727.
11. Hafizovic, J.; Bjørgen, M.; Olsbye, U.; Dietzel, P. D. C.; Bordiga, S.; Prestipino, C.; Lamberti, C.; Lillerud, K. P. *J. Am. Chem. Soc.* **2007**, *129*, 3612–3620.
12. Huang, L.; Wang, H.; Chen, J.; Wang, Z.; Sun, J.; Zhao, D.; Yan, Y. *Microporous Mesoporous Mater.* **2003**, *58*, 105–114.
13. Wang, Y.; Lin, F.; Pang, W. *J. Coord. Chem.* **2006**, *59*, 499–504.
14. Rosi, N. L.; Kim, J.; Eddaoudi, M.; Chen, B.; O'Keeffe, M.; Yaghi, O. M. *J. Am. Chem. Soc.* **2005**, *127*, 1504–1518.
15. Chae, H. K.; Siberio-Perez, D. Y.; Kim, J.; Go, Y.-B.; Eddaoudi, M.; Matzger, A. J.; O'Keeffe, M.; Yaghi, O. M. *Nature* **2004**, *427*, 523–527.
16. Chui, S. S.-Y.; Lo, S. M.-F.; Charmant, J. P. H.; Orpen, A. G.; Williams, I. D. *Science* **1999**, *283*, 1148–1150.
17. Wong-Foy, A.; Matzger, A. J.; Yaghi, O. M. *J. Am. Chem. Soc.* **2006**, *128*, 3494–3495.
18. Li, J.; Brill, T. B. *J. Phys. Chem. A* **2002**, *106*, 9491–9498.
19. Kim, J.; Chen, B.; Reineke, T. M.; Li, H.; Eddaoudi, M.; Moler, D. B.; O'Keeffe, M.; Yaghi, O. M. *J. Am. Chem. Soc.* **2001**, *123*, 8239–8247.
20. *Cerius*^{2} *Modeling Environment, Version 4.2*; Molecular Simulations: San Diego, CA, 1999.
21. Reineke, T.; Eddaoudi, M.; Moler, D.; O'Keeffe, M.; Yaghi, O. M. *J. Am. Chem. Soc.* **2000**, *122*, 4843–4844.
22. Kesanli, B.; Cui, Y.; Smith, M. R.; Bittner, E. W.; Bockrath, B. C.; Lin, W. *Angew. Chem., Int. Ed.* **2005**, *44*, 72–75.
23. Leban, I. *Cryst. Struct. Commun.* **1974**, *3*, 241–243.
24. Kraus, W.; Nolze, G. *J. Appl. Crystallogr.* **1996**, *29*, 301–303.